Electronic Supplementary Material (ESI) for Polymer Chemistry.
This journal is © The Royal Society of Chemistry 2023

Supporting Information

Solid State Chemical Transformation Provides a Fully Benzoxazine-Linked Porous Organic Polymer Displaying Enhanced CO_2 Capture and Supercapacitor Performance

Mohsin Ejaz,[a] Mohamed Gamal Mohamed[a,b]*, and Shiao-Wei Kuo[a,c]*

[a]Department of Materials and Optoelectronic Science, Center for Functional Polymers and Supramolecular Materials, National Sun Yat-Sen University, Kaohsiung 804, Taiwan.

[b]Chemistry Department, Faculty of Science, Assiut University, Assiut 71515, Egypt.

[c]Department of Medicinal and Applied Chemistry, Kaohsiung Medical University, Kaohsiung 807, Taiwan

Corresponding authors: mgamal.eldin12@yahoo.com (M. G. Mohamed) and (kuosw@faculty.nsysu.edu.tw (S. W. Kuo)

Characterization

FTIR spectra were collected using a Bruker Tensor 27 FTIR spectrophotometer at a resolution of 4 cm^{-1} and the KBr disk method. ^{13}C nuclear magnetic resonance (NMR) spectra were recorded using an INOVA 500 instrument, with DMSO as the solvent and tetramethylsilane (TMS) as the external standard; chemical shifts are reported in parts per million (ppm). The thermal stabilities of the samples under N_2 were measured using a TG Q-50 thermogravimetric analyzer; the cured sample (ca. 5 mg) was placed in a Pt cell and then heated at 20 °C min^{-1} from 100 to 800 °C under a N_2 flow of 60 mL min^{-1}. Wide-angle X-ray diffraction (WAXD) patterns were measured at the wiggler beamline BL17A1 of the National Synchrotron Radiation Research Center (NSRRC), Taiwan; a triangular bent Si (111) single crystal was used to obtain a monochromated beam having a wavelength (λ) of 1.33 Å. The morphologies of the polymer samples were examined through field emission scanning electron microscopy (FE-SEM; JEOL JSM7610F) and transmission electron microscopy (TEM), using a JEOL-2100 microscope operated at an accelerating voltage of 200 kV. BET surface areas and porosimetry measurements of the samples (ca. 40–100 mg) were performed using a BEL Master™ instrument and BEL sim™ software (v. 3.0.0); N_2 adsorption and desorption isotherms were generated through incremental exposure to ultrahigh-purity N_2 (up to ca. 1 atm) in a liquid N_2 (77 K) bath; surface parameters were calculated using the BET adsorption models in the instrument's software. The pore sizes of the prepared samples were determined using nonlocal density functional theory (NLDFT).

Electrochemical Analysis

Working Electrode Cleaning: Prior to use, the glassy carbon electrode (GCE) was polished several times with 0.05-μm alumina powder, washed with EtOH after each polishing step, cleaned through sonication (5 min) in a water bath, washed with EtOH, and then dried in air.

Electrochemical Characterization: The electrochemical experiments were performed in a three-electrode cell using an Autolab potentiostat (PGSTAT204) and 1 M KOH as the aqueous electrolyte. The GCE was used as the working electrode (diameter: 5.61 mm; 0.2475 cm^2); a Pt wire was used as the counter electrode; Hg/HgO (RE-1B, BAS) was the reference electrode. All reported potentials refer to the Hg/HgO potential. A slurry was prepared by dispersing the TPA-DHTP-BZ POP or poly(TPA-DHTP-BZ) POP sample (45 wt. %), carbon black (45 wt. %), and Nafion (10 wt. %) in a mixture of (EtOH/ H_2O) (200 µL: 800 µL) and then sonicated for 1 h. A portion of this slurry (10 µL) was pipetted onto the tip of the electrode, which was then dried in air for 30 min prior to use. The electrochemical performance was studied through CV at various sweep rates (5–200 mV s^{-1}) and through the GCD method in the potential range from 0 to –1.00 V (vs. Hg/HgO) at various current densities (0.5–20 A g^{-1}) in 1 M KOH as the aqueous electrolyte solution.

The specific capacitance was calculated from the GCD data using the equation:

$$C_s = (I\Delta t)/(m\Delta V)$$

Where C_s (F g^{-1}) is the specific capacitance of the supercapacitor, I (A) is the discharge current, ΔV (V) is the potential window, Δt (s) is the discharge time, and m (g) is the mass of the NPC on the electrode. The energy density (E, W h kg^{-1}) and power density (P, W kg^{-1}) were calculated using the equations.

$$E = 1000C(\Delta V)^2/(2 \times 3600)$$

$$P = E/(t/3600)$$

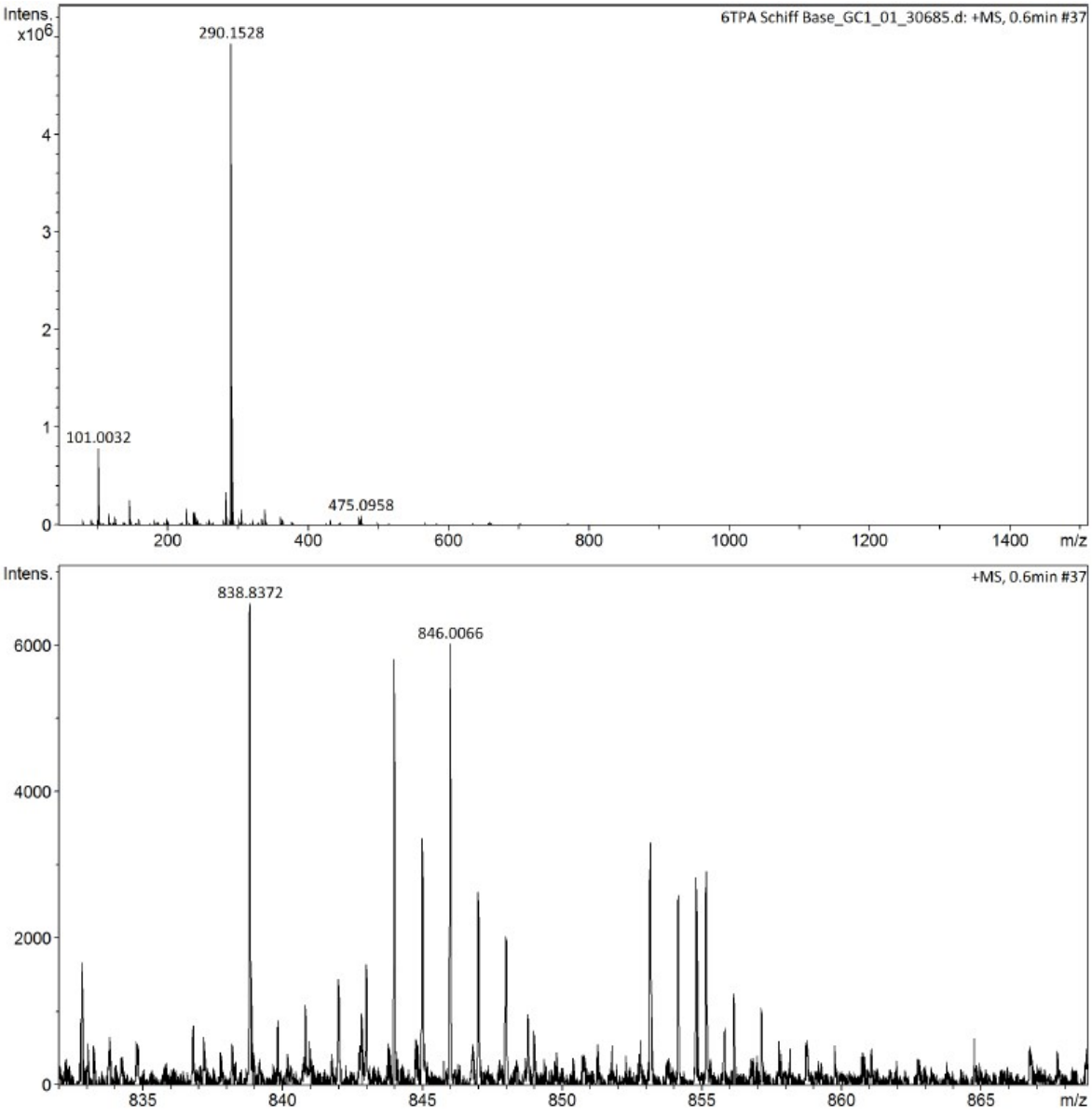

Figure S1. High-resolution mass spectrum of TPA-SB-Br.

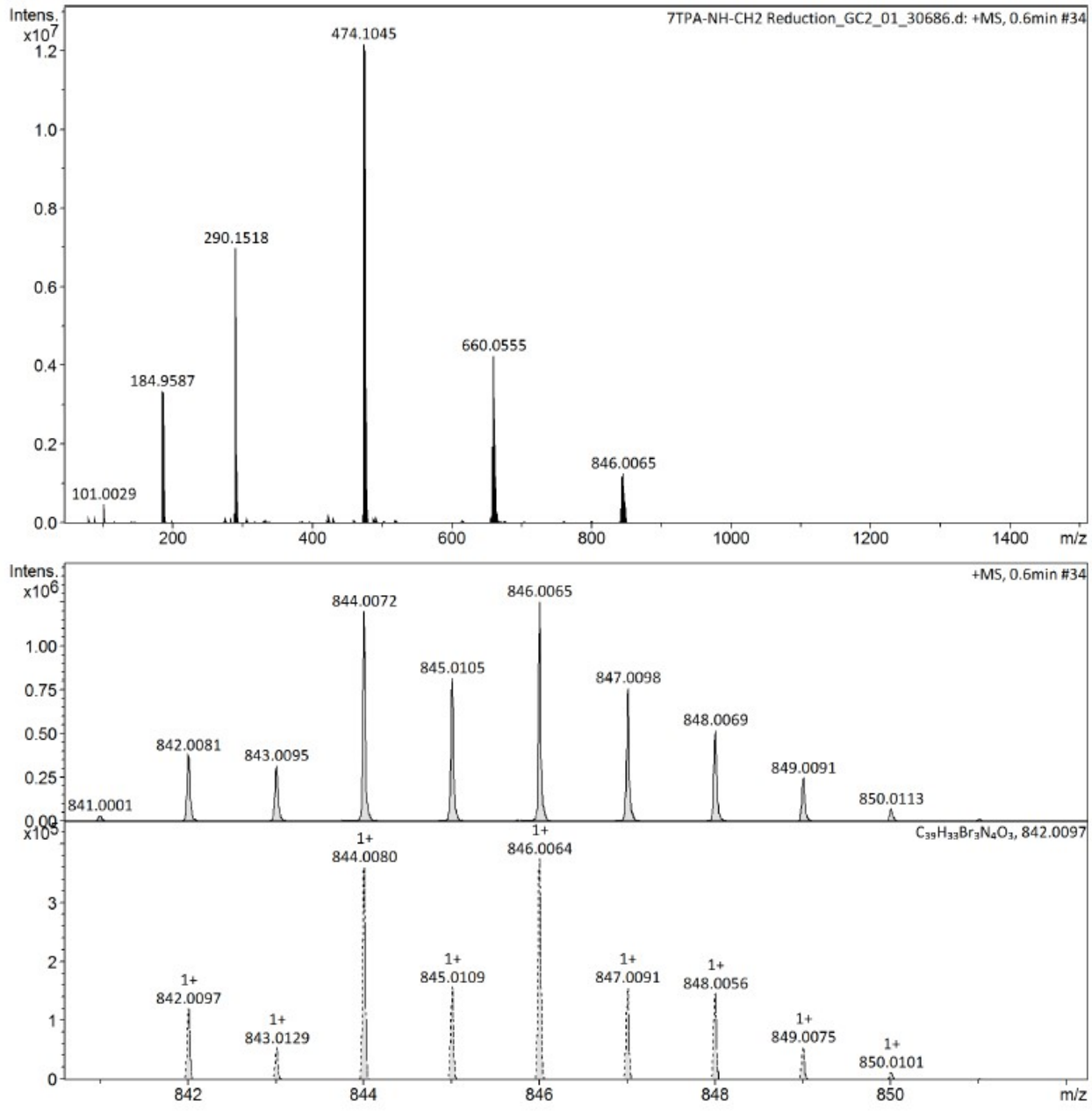

Figure S2. High-resolution mass spectrum of TPA-R-Br.

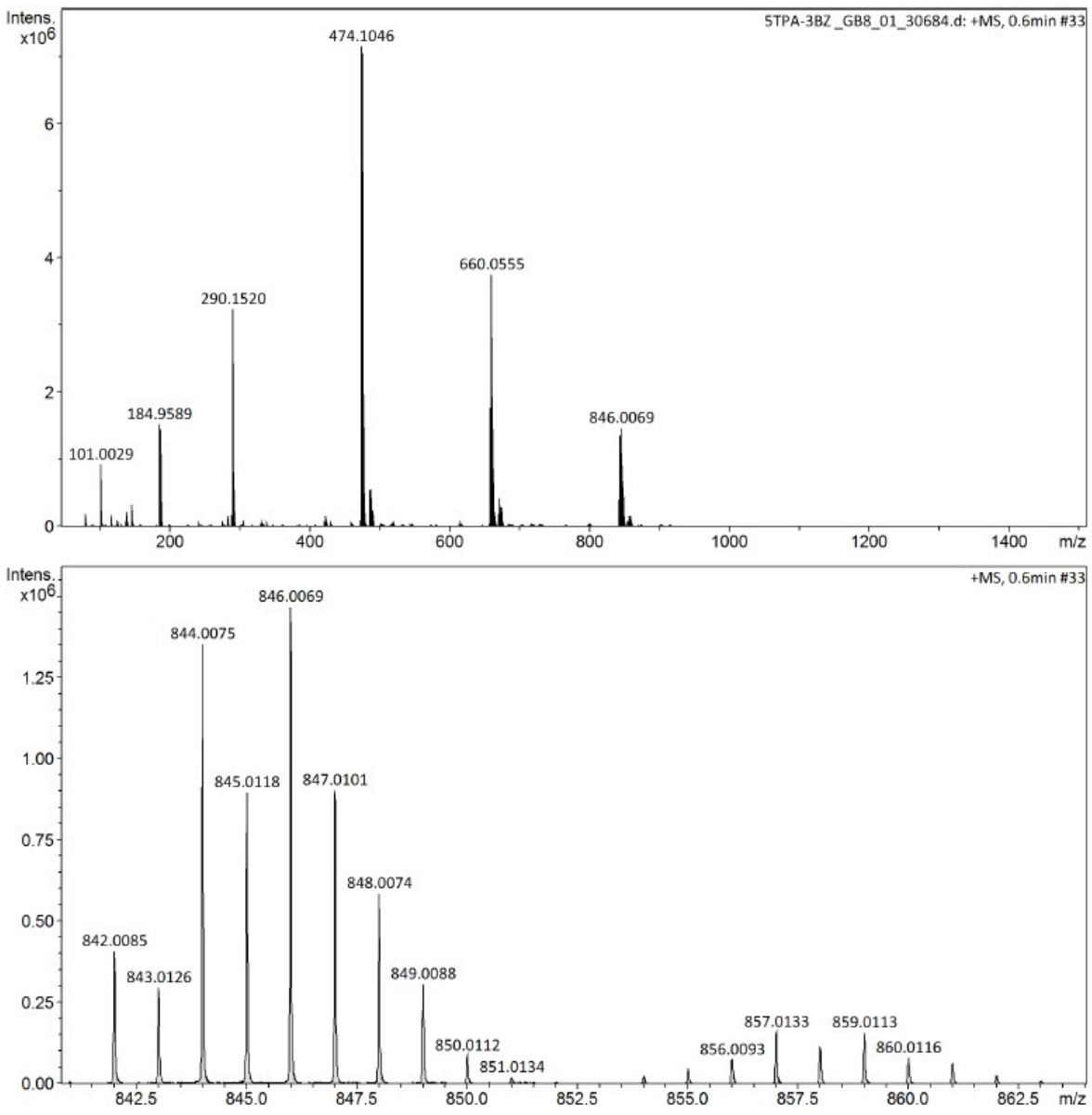

Figure S3. High-resolution mass spectrum of TPA-Br-BZ.

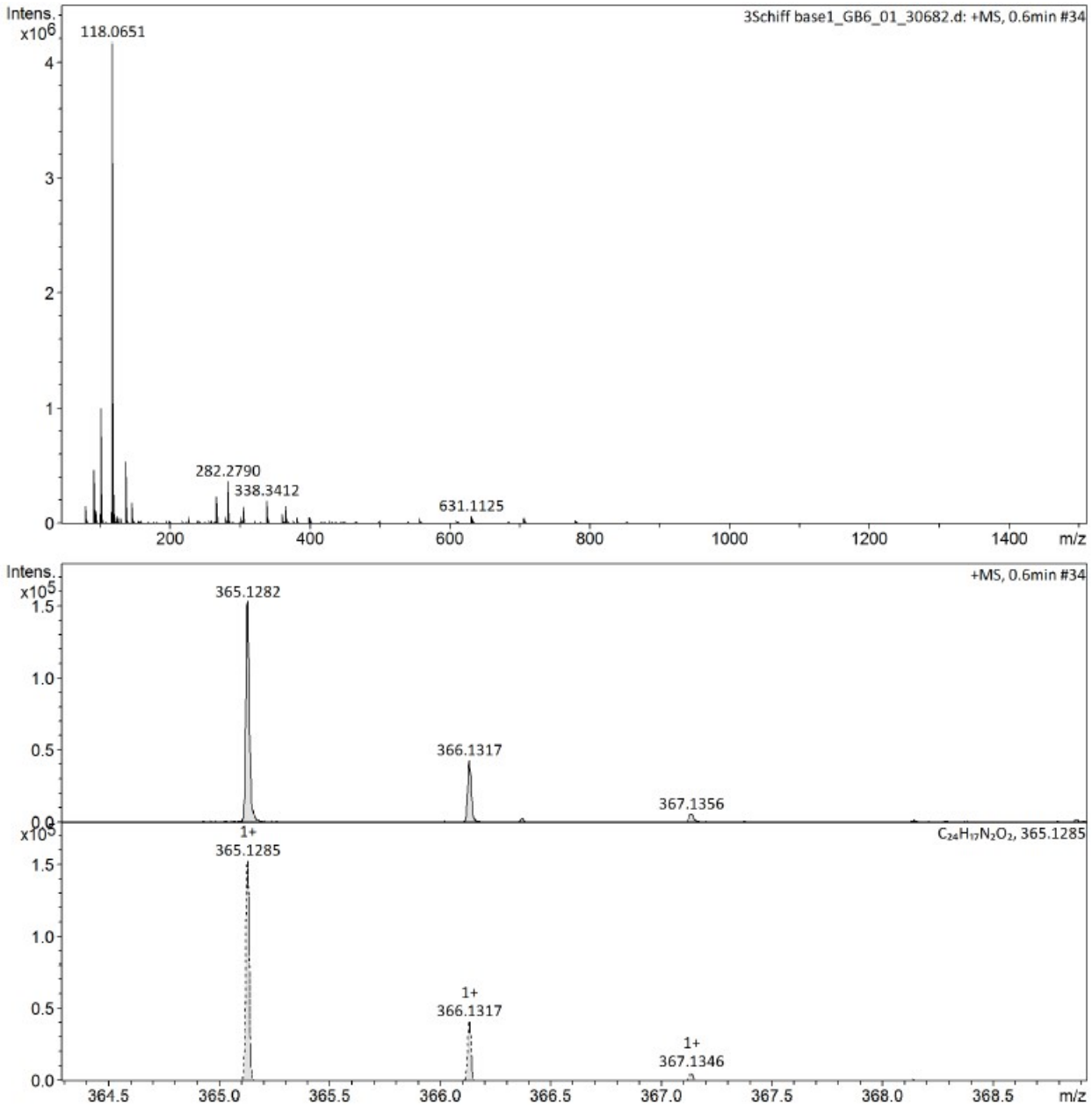

Figure S4. High-resolution mass spectrum of DHTP-SB-Ea.

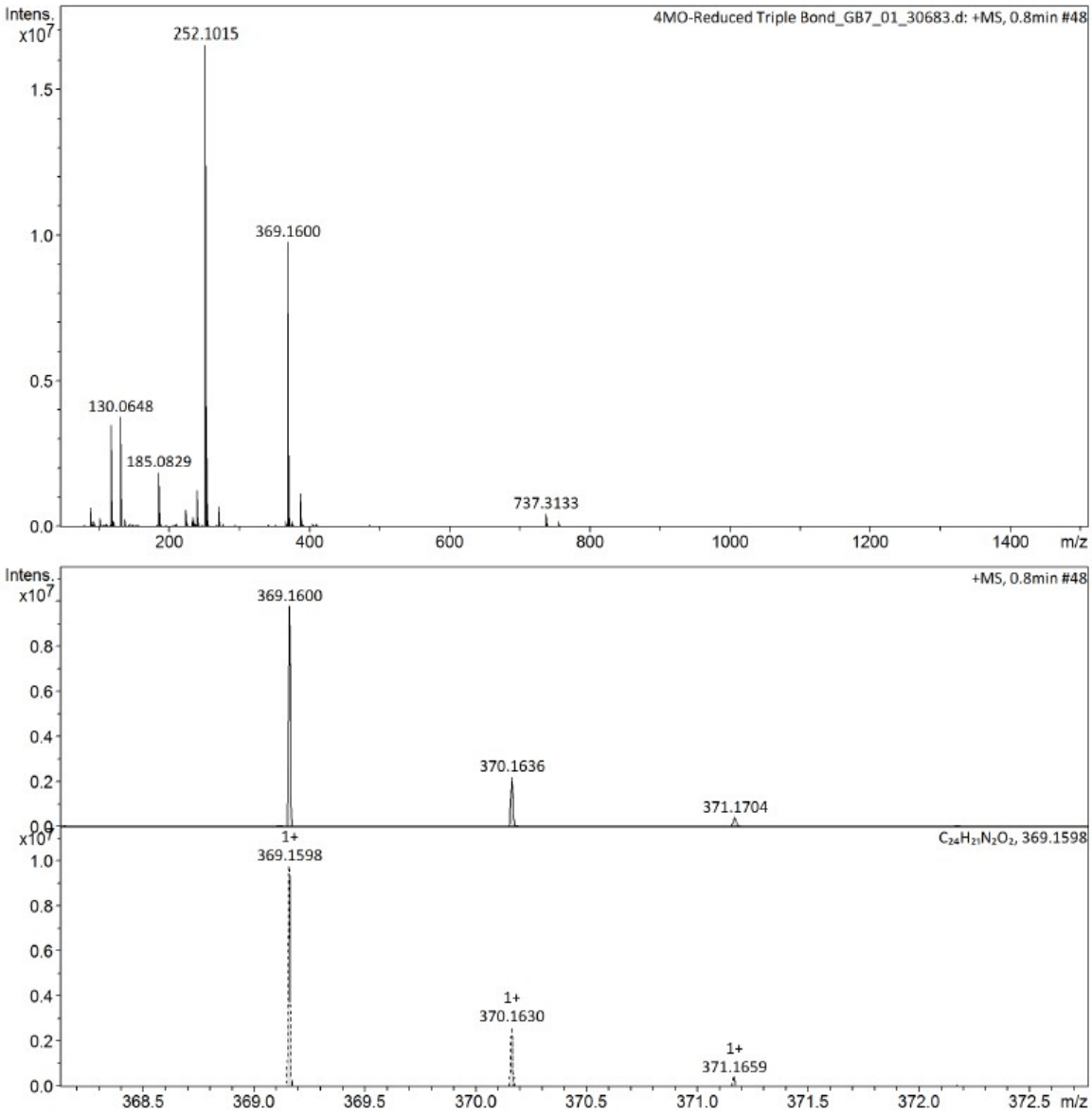

Figure S5. High-resolution mass spectrum of DHTP-R-Ea.

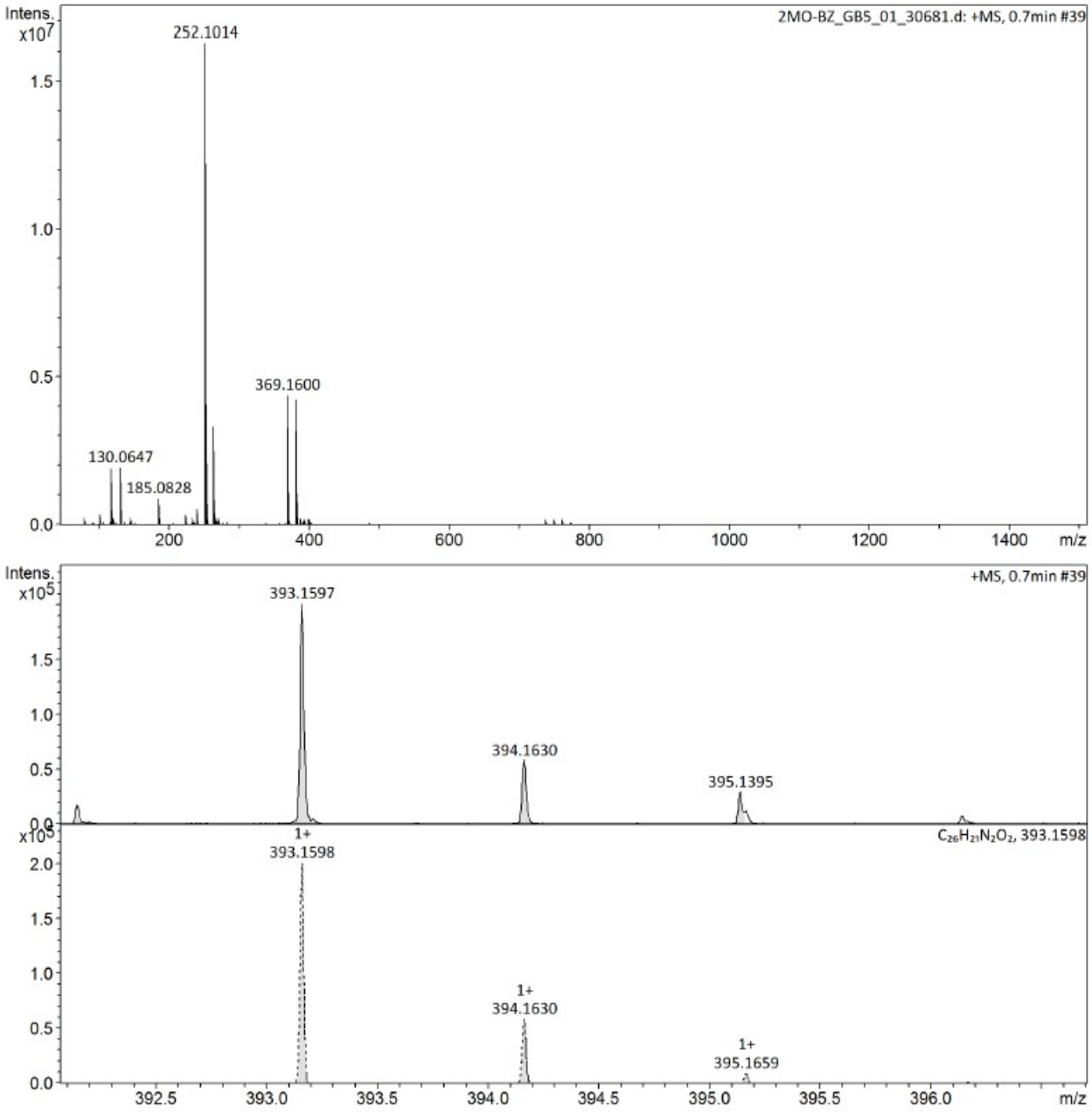

Figure S6. High-resolution mass spectrum of DHTP-Ea BZ.

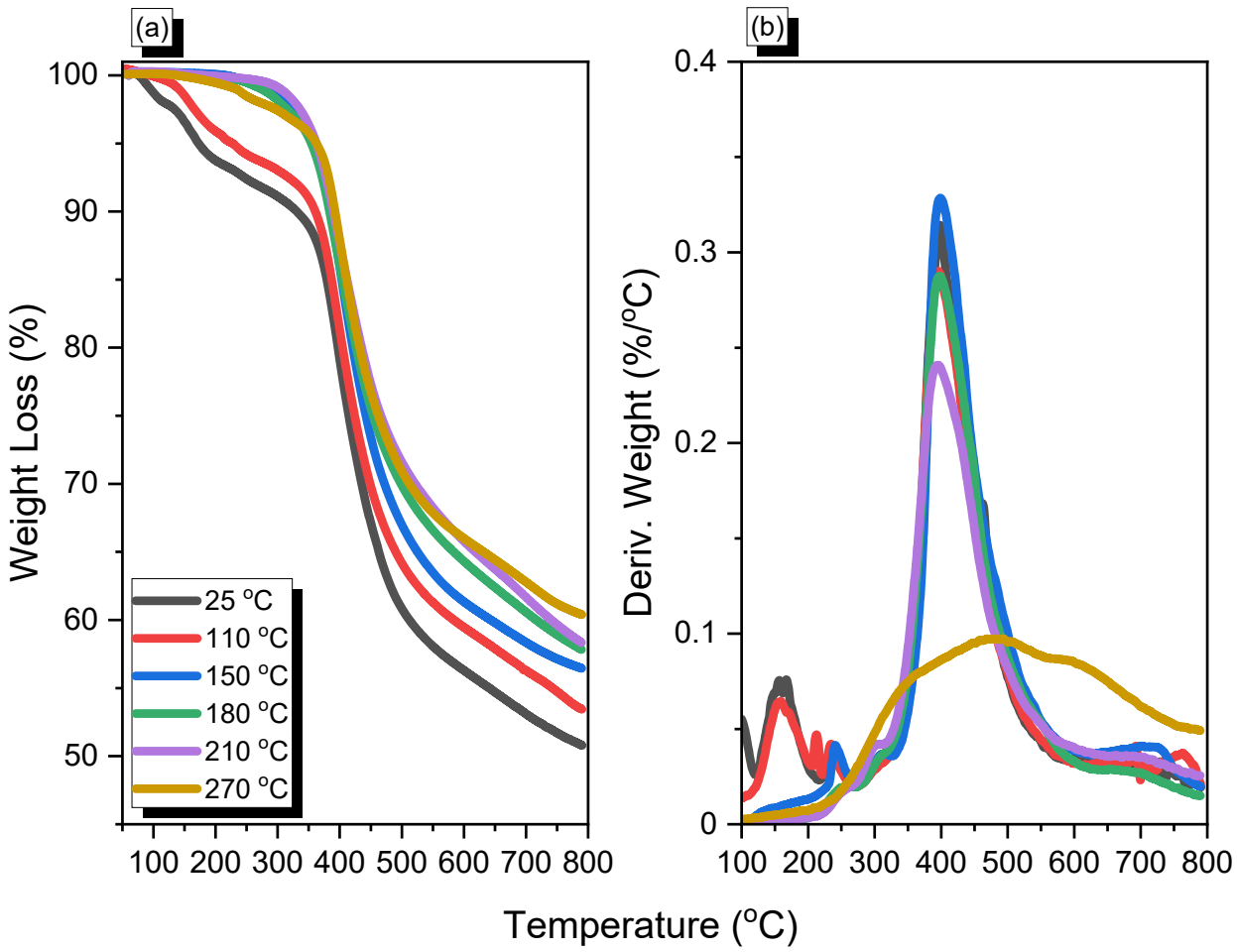

Figure S7. (a) TGA (c) and (b) second-derivative based on TGA analyses of the TPA-Br-BZ before and after thermal ROP at various temperatures.

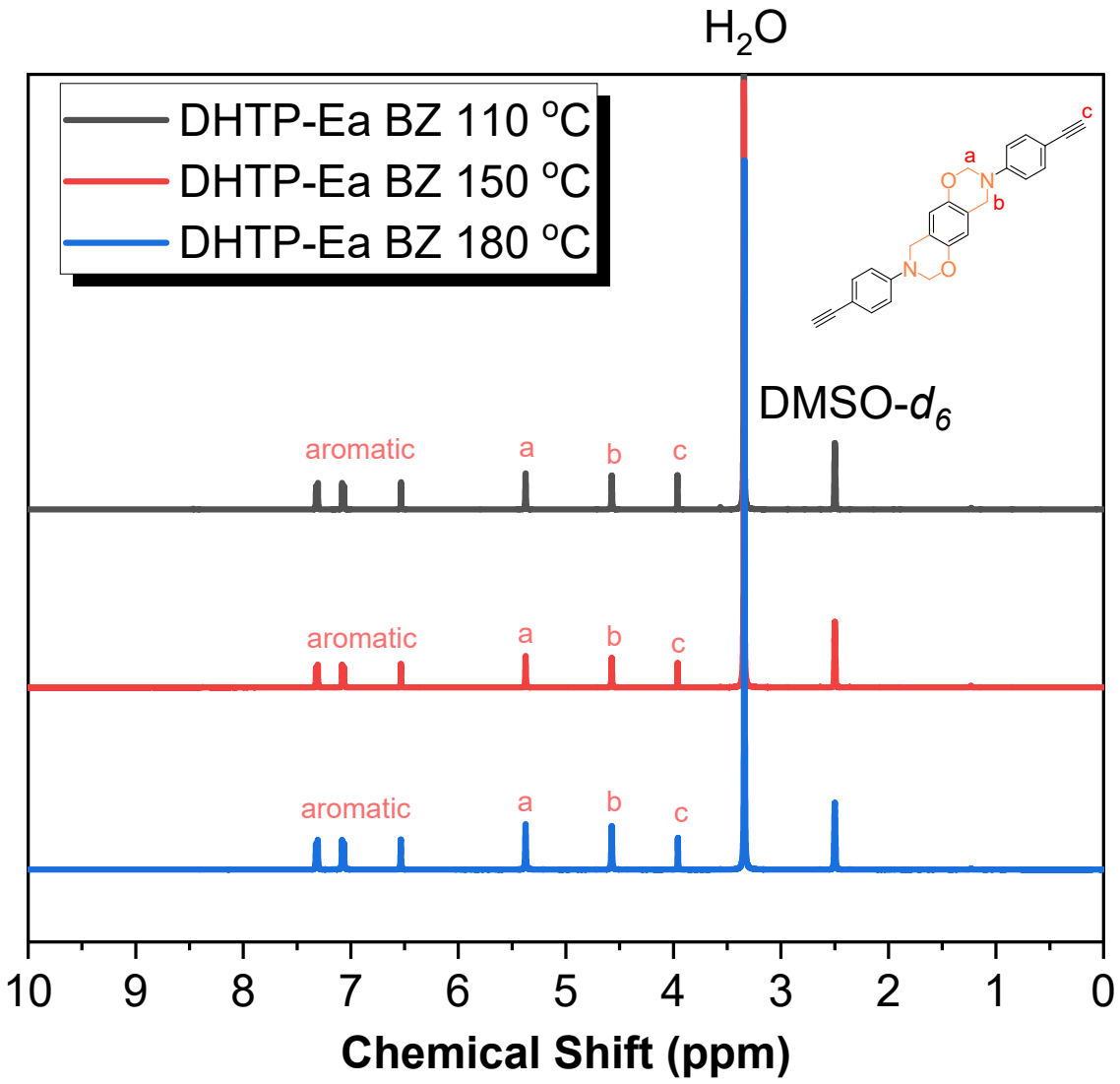

Figure S8. ^{1}H-NMR profiles of DHTP-Ea BZ after thermal treatment at 110, 150, and 180 °C.

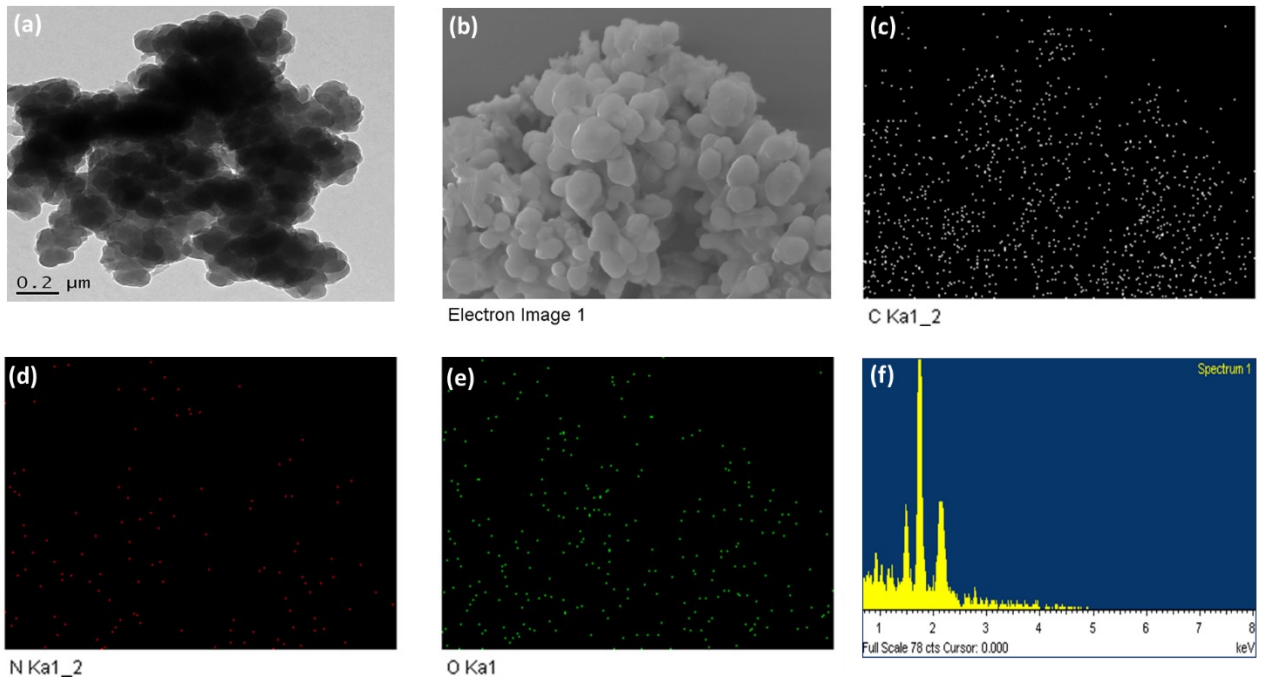

Figure S9. (a) TEM and (b) SEM images of the TPA-DHTP-BZ POP. (c–f) Corresponding (c) C-, (d) N-, and (e) O-mapping and (f) EDX analyses.

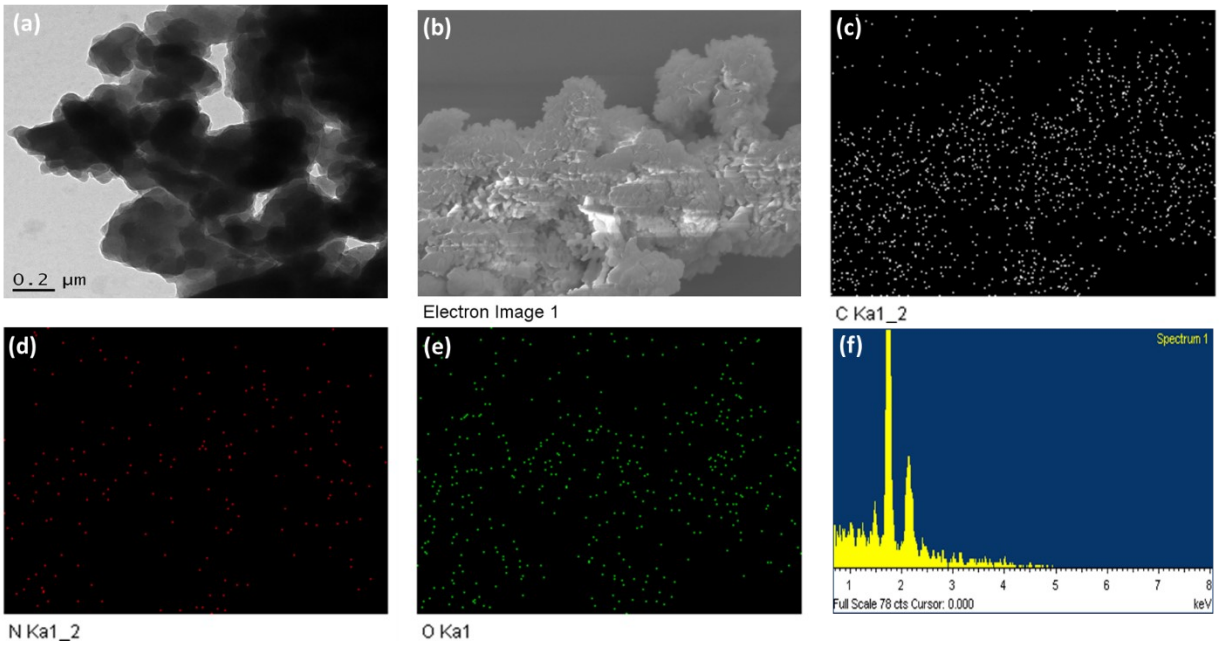

Figure S10. (a) TEM and (b) SEM images of the poly(TPA-DHTP-BZ) POP. (c–f) Corresponding (c) C-, (d) N-, and (e) O-mapping and (f) EDX analyses.

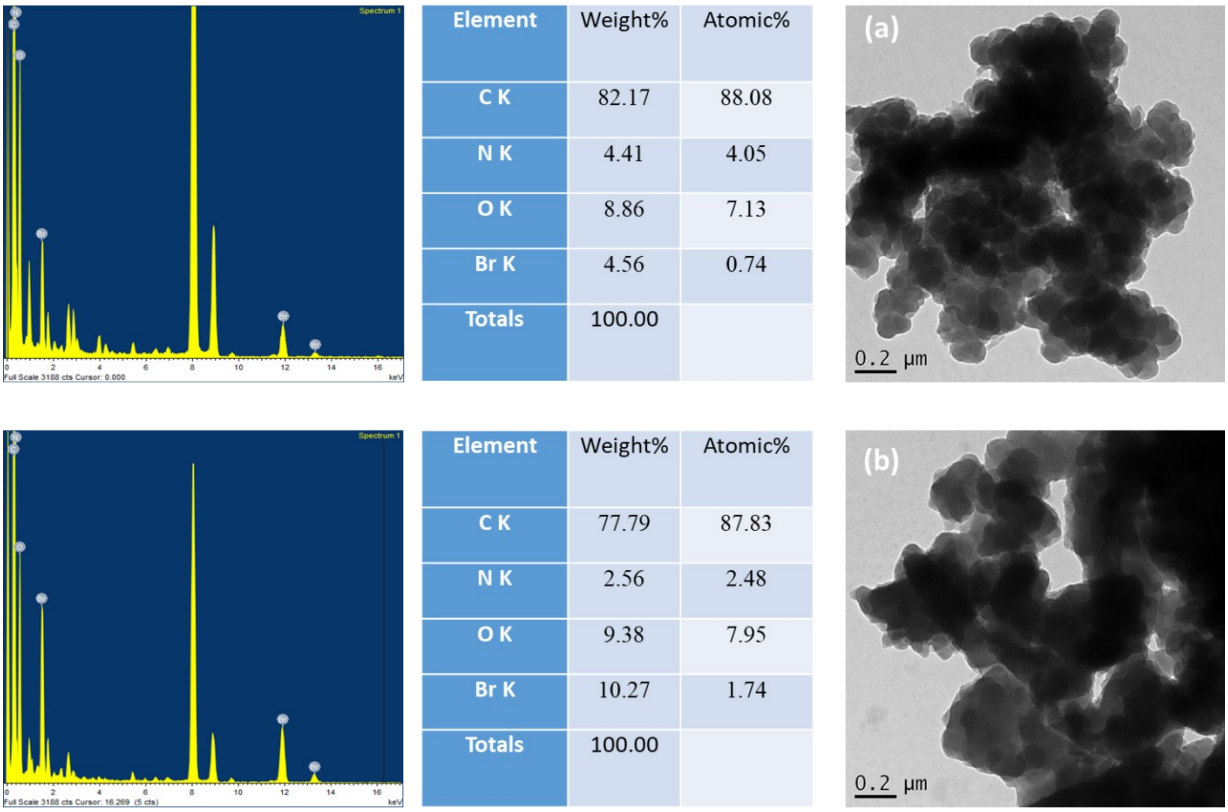

Figure S11. TEM images and EDX analyses with element contents of the TPA-DHTP-BZ POP (a) and poly(TPA-DHTP-BZ) POP (b).

Table S1. Comparison of TPA-DHTP-BZ POP and poly(TPA-DHTP-BZ) POP for CO_2 uptake with other porous materials.

Sample	CO_2 uptake (mmol/g)	Ref.
TPA-DHTP-BZ POP	0.97	This work
Poly(TPA-DHTP-BZ) POP	3.29	This work
RLF-500	3.13	S1
ELF6	3.29	S2
ELF46	2.46	S2
ELF56	2.98	S2
BZPh-A	1.44	S3
BZPh-CN-A	2.28	S3
poly(Py-TPE-BZ)	2.2	S4
poly(TPE-TPE-BZ)	2.21	S4
BPOP-1	0.98	S5
BPOP-2	0.67	S5
BoxPOP-1	0.91	S6
BoxPOP-2	1.04	S6
BoxPOP-3	0.29	S6

Table S2. Comparison between the specific capacitance of TPA-DHTP-BZ POP and poly(TPA-DHTP-BZ) POP with those of previously reported materials for supercapacitor application.

Electrode	Capacitance	Ref.
TPA-DHTP-BZ POP	31.37 F g^{-1} at 0.5 A g^{-1}	This work
Poly(TPA-DHTP-BZ) POP	67.06 F g^{-1} at 0.5 A g^{-1}	This work
Cz-Cz CMP	43.70 F g^{-1} at 0.5 A g^{-1}	S7
Cz-TP CMP	67.38 F g^{-1} at 1 A g^{-1}	S7
POSS-F-POIP	36.2 F g^{-1} at 0.5 A g^{-1}	S8
H-THAQ	15 F g^{-1} at 1 A g^{-1}	S9
THAQ/rGO (2:1)	76 F g^{-1} at 1 A g^{-1}	S9
Pure AQ	42 F g^{-1} at 1 A g^{-1}	S10
TPE-DDSQ-POIP	22 F g^{-1} at 1 A g^{-1}	S11
Car-DDSQ-POIP	23 F g^{-1} at 1 A g^{-1}	S11
N- doped Porous carbons ropes	60 F g^{-1} at 1.0 A g^{-1}	S12
TPE-FFC-CMP/CD-BZ	7.53 at 0.5 A g^{-1}	S13
TPE-FFC-CMP/poly (CD-BZ)	37.07 at 0.5 A g^{-1}	S13
Py-FFC-CMP/CD-BZ	10.15 at 0.5 A g^{-1}	S13
Py-FFC-CMP/poly (CD-BZ)	46 at 0.5 A g^{-1}	S13
HPC-0	48 at 1 A g^{-1}	S14
H-THAQ	15 F g–1 at 1 A g^{-1}	S15

References

[S1] Hao, G. P.; Li, W. C.; Qian, D.; Lu, A. H. Rapid synthesis of nitrogen-doped Porous Carbon Monolith for CO_2 Capture. *Adv. Mater*. **2010**, *22*, 853−857. doi.org/10.1002/adma.200903765

[S2] Shi, W.; Zhang, X.; Ji, Y.; Zhao, Z.; Li, W.; Jia, X. Sustainable Preparation of Bio-Based Polybenzoxazine Resins from Amino Acid and Their Application in CO_2 Adsorption. *ACS Sustainable Chem. Eng*. **2019**, *7*, 17313-17324. doi.org/10.1021/acssuschemeng.9b04163.

[S3] Wu, J.-Y.; Mohamed, G. M.; Kuo, S.-W. Directly synthesized nitrogen-doped microporous carbons from polybenzoxazine resins for carbon dioxide capture. *Polym. Chem.* **2017**, *8*, 5481–5489. DOI: 10.1039/c7py01026e.

[S4] Mohamed, M. G.; Chen, T. C.; Kuo, S. W. Solid-State Chemical Transformations to Enhance Gas Capture in Benzoxazine-Linked Conjugated Microporous Polymers. *Macromolecules* **2021**, *54*, 5866–5877. DOI: 10.1021/acs.macromol.1c00736.

[S5] Sun, X.; Li, J.; Wang, W.; Ma, Q. Constructing Benzoxazine-Containing Porous Organic Polymers for Carbon Dioxide and Hydrogen Sorption. *Eur. Polym. J.* **2018**, *107*, 89–95. DOI: 10.1016/j.eurpolymj.2018.07.043.

[S6] Xu, S.; He, J.; Jin, S.; Tan, B. Heteroatom-Rich Porous Organic Polymers Constructed by Benzoxazine Linkage with High Carbon Dioxide Adsorption Affinity. *J. Colloid Interface Sci.* **2018**, *509*, 457–462. DOI: 10.1016/j.jcis.2017.09.009.

[S7] Saber, A. F.; Sharma, S. U.; Lee, J. T.; EL-Mahdy, A. F. M.; Kuo, S. W. Carbazole-conjugated microporous polymers from Suzuki–Miyaura coupling for supercapacitors. *Polymer*, **2022**, *254*, 125070. doi.org/10.1016/j.polymer.2022.125070.

[S8] Mohamed, M.G.; Mansoure, T.H.; Takashi, Y.; Samy, M.M.; Chen, T.; Kuo, S.-W. Ultrastable porous organic/inorganic polymers based on polyhedral oligomeric silsesquioxane (POSS) hybrids exhibiting high performance for thermal property and energy storage. *Microporous Mesoporous Mater.* **2021**, *328*, 111505. doi.org/10.1016/j.micromeso.2021.111505.

[S9] Xu, L.; Shi, R.; Li, H.; Han, C.; Wu, M.; Wong, C.P. Kang, F.; Li, B. Pseudocapacitive anthraquinone modified with reduced graphene oxide for flexible symmetric all-solid-state supercapacitors. *Carbon*, **2018**, *127*, 459-468. doi.org/10.1016/j.carbon.2017.11.003.

[S10] Guo, B.; Yang, Y.; Hu, Z.; An, Y.; Zhang, Q.; Yang, X.; Wang, X.; Wu, H. Redox-active organic molecules functionalized nitrogen-doped porous carbon derived from metal-organic framework as electrode materials for supercapacitor. *Electrochim. Acta,* **2017**, *223*, 74–84. doi.org/10.1016/j.electacta.2016.12.012.

[S11] Mohamed, M.G.; Chen, W.C; Mahdy, A.F.M.; Kuo, S.W. Porous organic/inorganic polymers based on double-decker silsesquioxane for high-performance energy storage*, J. Polym. Res.* **2021**, *28*, 219. doi.org/10.1007/s10965-021-02579-x.

[S12] Thirukumaran, P.; Parven, A.; Lee, Y. R.; Kim, S. C. Polybenzoxazine originated N-doped mesoporous carbon ropes as an electrode material for high-performance supercapacitors. *J. Alloys Comp*., **2018**, *750*, 384-391. doi.org/10.1016/j.jallcom.2018.04.034.

[S13] Samy, M. M.; Mohamed, M. G.; Mansoure, T. H.; Meng, T. S.; Khan, M. A. R.; Liaw, C. C.; Kuo, S. W. Solid state chemical transformations through ring-opening polymerization of ferrocene-based conjugated microporous polymers in host–guest complexes with benzoxazine-linked cyclodextrin. *J. Taiwan Inst. Chem. Eng.*, **2022**, *132*, 104110. DOI: 10.1016/j.jtice.2021.10.010.

[S14] Wan, L.; Wang, J.; Xie, L.; Sun, Y; Li, K. Nitrogen-enriched hierarchically porous carbons prepared from polybenzoxazine for high-performance supercapacitors. *ACS Appl. Mater. Interfaces,* **2014**, *6*, 15583–15596. DOI: 10.1021/am504564q.

[S15] Xu, L.; Shi, R.; Li, H.; Han, C.; Wu, M.; Wong, C.P.; Kang, F.; Li, B. Pseudocapacitive anthraquinone modified with reduced graphene oxide for flexible symmetric all-solid-state supercapacitors. *Carbon,* **2018**; *127*, 459-68. DOI: 10.1016/j.carbon.2017.11.003.